JOHANNES GUTENBERG UNIVERSITÄT MAINZ

The (g-2) intermediate window quantity from a coordinate-space method

En-Hung Chao, Harvey Meyer, Julian Parrino

Lattice 2022, Bonn, 8-13 August 2022

The (g-2) intermediate window quantity

The (g-2) intermediate window quantity

Motivation

$$\boldsymbol{\mu} = g\frac{e}{2m}\boldsymbol{s}, \qquad a = \frac{g-2}{2} \tag{1}$$

- Since Fermilab experiment (2021):
  - 4.2σ tension between experiment and combined theory value (white paper [2006.04822])

Main uncertainty comes from hadronic vacuum polarization

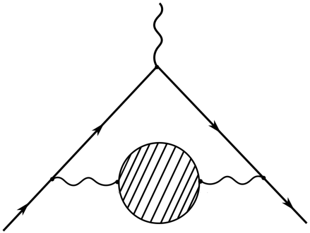

The (g-2) intermediate window quantity

2 branches of theoretical calculations:

- Dispersive approach:
  (see e.g. Jegerlehner, Nyffeler [0902.3360])

$$a_\mu^{\mathrm{HVP,LO}} = \frac{\alpha^2}{3\pi^2} \int_{m_\pi^2}^{\infty} \frac{K(s)}{s} R(s)\, ds, \qquad R(s) = \frac{\sigma(e^+e^- \to \mathrm{hadrons}(+\gamma))}{\left(4\pi\alpha^2/(3s)\right)} \tag{2}$$

- Lattice determination:
  (Time-momentum representation (TMR), Bernecker, Meyer [1107.4388])

$$a_\mu^{\mathrm{HVP,LO}} = \left(\frac{\alpha}{\pi}\right)^2 \int_0^{\infty} f(t, m_\mu) G(t)\, dt, \qquad G(t) = -\frac{1}{3} \sum_{i=1}^{3} \int \langle j_i(x) j_i(0) \rangle\, d^3x \tag{3}$$

$$j_\mu(x) = \frac{2}{3}\bar{u}(x)\gamma_\mu u(x) - \frac{1}{3}\bar{d}(x)\gamma_\mu d(x) - \frac{1}{3}\bar{s}(x)\gamma_\mu s(x) + \ldots \tag{4}$$

The (g-2) intermediate window quantity

2 branches of theoretical calculations:

- Dispersive approach: $a_\mu^{\mathrm{HVP,LO}} = 693.1(40)x10^{-10}$ [2006.04822]
  (see e.g. Jegerlehner, Nyffeler [0902.3360])

$$a_\mu^{\mathrm{HVP,LO}} = \frac{\alpha^2}{3\pi^2}\int_{m_\pi^2}^{\infty} \frac{K(s)}{s} R(s)\, ds, \qquad R(s) = \frac{\sigma(e^+e^- \to \mathrm{hadrons}(+\gamma))}{\left(4\pi\alpha^2/(3s)\right)} \tag{5}$$

- Lattice determination: $a_\mu^{\mathrm{HVP,LO}} = 711.6(184)x10^{-10}$ [2006.04822]
  (Time-momentum representation (TMR), Bernecker, Meyer [1107.4388])

$$a_\mu^{\mathrm{HVP,LO}} = \left(\frac{\alpha}{\pi}\right)^2 \int_0^{\infty} f(t, m_\mu) G(t)\, dt, \qquad G(t) = -\frac{1}{3}\sum_{i=1}^{3}\int \langle j_i(x) j_i(0)\rangle\, d^3x \tag{6}$$

$$j_\mu(x) = \frac{2}{3}\bar{u}(x)\gamma_\mu u(x) - \frac{1}{3}\bar{d}(x)\gamma_\mu d(x) - \frac{1}{3}\bar{s}(x)\gamma_\mu s(x) + \ldots \tag{7}$$

The (g-2) intermediate window quantity

Define benchmark quantity:

$$a_\mu^{\mathrm{win}} = \int_0^\infty f_W(t, m_\mu) G(t)\, dt \qquad (8)$$

$$t_0 = 0.4fm, \quad t_1 = 1.0fm, \quad \Delta = 0.15fm$$

$$f_W(t, m_\mu) = \left(\frac{\alpha}{\pi}\right)^2 (\theta_\Delta(t - t_0) - \theta_\Delta(t - t_1)) \cdot f(t, m_\mu)$$

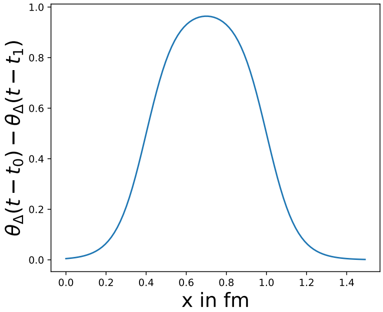

- Reduced cut-off effects and finite-volume artifacts on the lattice

The (g-2) intermediate window quantity

Results so far

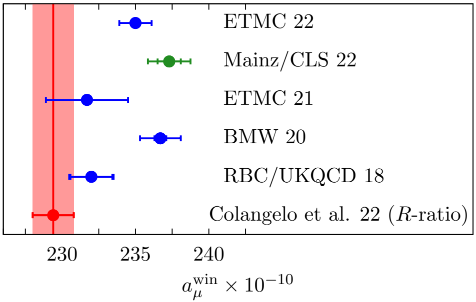

(a) Results for the window quantity from different lattice calculations → Talk by Simon Kuberski

- Overall good agreement between different lattice calculations
- But, all rely on the time-momentum representation
- TMR method is a calculation in the $\boldsymbol{p} = 0$ rest-frame
- Lattice breaks Lorentz symmetry, need to have a check that the symmetry is correctly restored in the continuum limit

Translating the window quantity to the covariant-coordinate space (CCS) method

Translating the window quantity to the CCS method

- CCS-representation, first derived by Meyer [1706.01139]
- A general weight function $f(t)$ in the TMR method, can be translated to the CCS-representation

$$a_\mu^{\mathrm{win}} = \int H_{\mu\nu}(x) G_{\mu\nu}(x)\, d^4x \tag{9}$$

$$H_{\mu\nu}(x) = -\delta_{\mu\nu}\mathcal{H}_1(|x|) + \frac{x_\mu x_\nu}{|x|^2}\mathcal{H}_2(|x|), \quad G_{\mu\nu}(x) = \langle j_\mu(x) j_\nu(0)\rangle \tag{10}$$

$$\mathcal{H}_1(|x|) = \frac{2}{9\pi|x|^4}\int_0^{|x|} dt \sqrt{|x|^2 - t^2}(2|x|^2 + t^2) f_W(t, m_\mu) \tag{11}$$

$$\mathcal{H}_2(|x|) = \frac{2}{9\pi|x|^4}\int_0^{|x|} dt \sqrt{|x|^2 - t^2}(4t^2 - |x|^2) f_W(t, m_\mu) \tag{12}$$

Freedom in the Choice of a Kernelfunction

- First shown in [1811.08669] by Cè at al. , use current conservation $\partial_\mu G_{\mu\nu} = 0$
  - Adding a total derivative to the kernel amounts a surface term

$$\widetilde{H}_{\mu\nu}(x) = H_{\mu\nu}(x) + \partial_\mu \Big(x_\nu g(|x|) \Big) \tag{13}$$

- Family of CCS-Kernels, which lead to the same integral in infinite volume

$$H^{\mathrm{TL}}_{\mu\nu}(x) = \Big(-\delta_{\mu\nu} + 4\frac{x_\mu x_\nu}{|x|^2} \Big) \mathcal{H}_2(|x|) \tag{14}$$

$$H^{\mathrm{XX}}_{\mu\nu}(x) = \frac{x_\mu x_\nu}{|x|^2} \Big(\mathcal{H}_2(|x|) + |x| \frac{d}{d|x|} \mathcal{H}_1(|x|) \Big) \tag{15}$$

Lattice Setup

Lattice Setup

Gauge ensembles

- We use 5 different CLS Ensembles at $m_\pi \sim 350$ MeV
- With $N_f = 2 + 1$ dynamical flavors of non-perturbatively $O(a)$ improved Wilson quarks and tree-level $O(a^2)$ improved Lüscher-Weisz gauge action
- 2 different discretizations of the vector current (local and conserved)

Id	β	$(\frac{L}{a})^3 \times (\frac{T}{a})$	a [fm]	m_π [MeV]	m_K [MeV]	$m_\pi L$	L [fm]	#confs light, strange
U102	3.4	$24^3 \times 96$	0.08636	353(4)	438(4)	3.7	2.1	200,0
H102		$32^3 \times 96$				4.9	2.8	240, 120
S400	3.46	$32^3 \times 128$	0.07634	350(4)	440(4)	4.2	2.4	240, 120
N203	3.55	$48^3 \times 128$	0.06426	346(4)	442(5)	5.4	3.1	90, 90
N302	3.7	$48^3 \times 128$	0.04981	346(4)	450(5)	4.2	2.4	240, 120

Finite Volume Correction

- Using Sakurai effective field theory [1101.2872]

$$\mathcal{L} = \frac{1}{4}F_{\mu\nu}(A)^2 + \frac{1}{4}F_{\mu\nu}(\rho)^2 + \frac{1}{2}m_\rho^2\rho_\mu^2 + \frac{e}{2g_\gamma}F_{\mu\nu}(A)F_{\mu\nu}(\rho) \quad (16)$$

$$+(D_\mu\pi)^\dagger(D_\mu\pi) + m_\pi^2\pi^\dagger\pi \quad (17)$$

with the covariant derivative $D_\mu = \partial_\mu - ieA_\mu - ig\rho_\mu$

- Prediction for the finite-volume effect agrees with the lattice data from the two ensembles with same parameters but different size

Features of the CCS-Method

Dependance of the integrand on the kernel

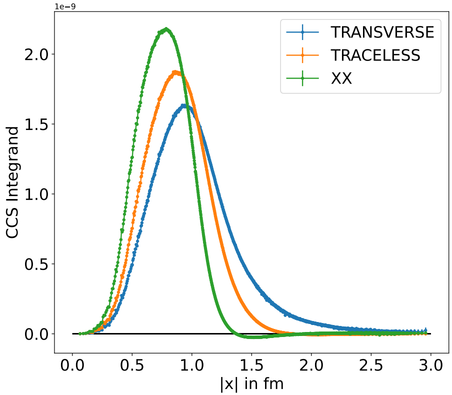

(a) Integrand of the CCS method for N203 (L=3.1 fm)

- Choice of the kernel affects the shape of the integrand
- Short ranged kernels are preferred
- But, might have unwanted oscillatory behaviour in the tail

Geometry of the domain of integration

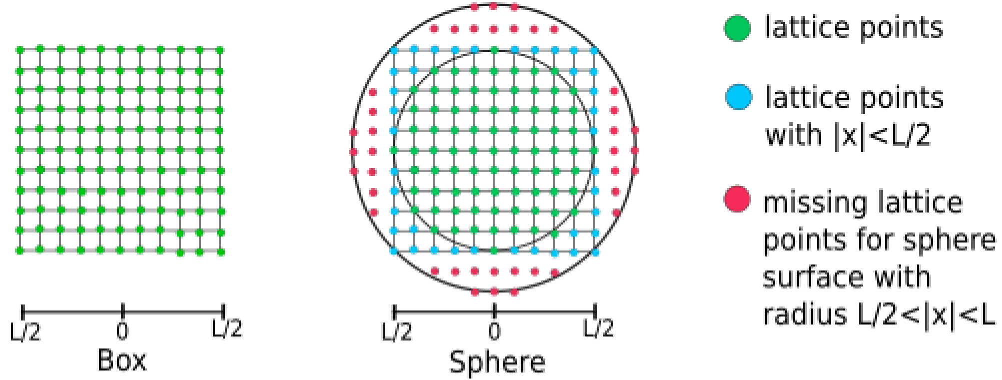

- For the blue points we need to compensate for the missing points by a correction factor ([1811.08669] Cè et al.)
- Effectively increasing integration length, but bad statistics for the tail

Results

Direct comparison between the TMR and CCS

- local-local currents

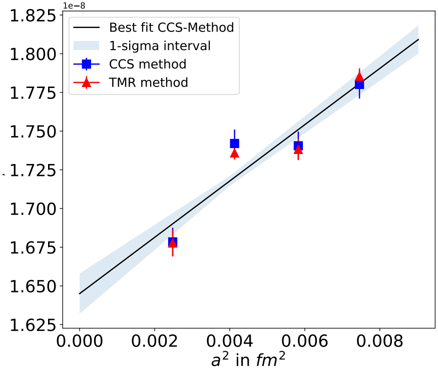

(a) Isovector contribution to a_μ^{win} at $m_\pi \sim 350$ MeV

- Finite volume corrections are applied to TMR and CCS results
- Ensembles are not exactly at the same pion mass $m_\pi \sim 346 - 353$ MeV
- Traceless Kernel chosen
- Integration in the Box
- Good agreement on each ensemble

Direct comparison between the TMR and CCS

- conserved-local currents

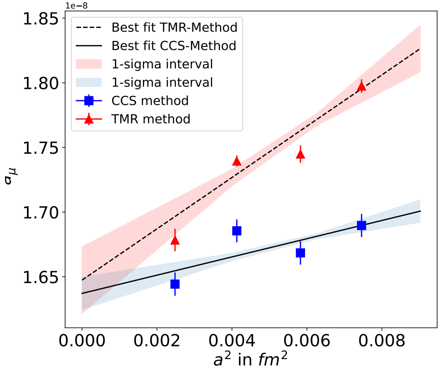

(a) Isovector contribution to a_μ^{win} at $m_\pi \sim 350$ MeV

- Finite volume corrections are applied to TMR and CCS results
- Ensembles are not exactly at the same pion mass $m_\pi \sim 346 - 353$ MeV
- Traceless Kernel chosen
- Integration in the Box
- Continuum result agrees

Setup for final results in the CCS method

- The traceless kernel is chosen
  - integrand is short ranged and oscillation in the tail is small
- We use the spherical integration domain
  - integration length can be effectively extended, which increases the precision on the small ensembles and leads to better continuum extrapolation
- Sakurai theory is used for finite-volume correction
- For the extrapolation to the physical pion mass, we use the best fit from the TMR method
  - Correction on each ensemble ($\sim 10\%$)

Continuum extrapolation at the physical pion mass

- Result for each value is corrected to the physical pion mass using the best global fit from the TMR method (small correction)

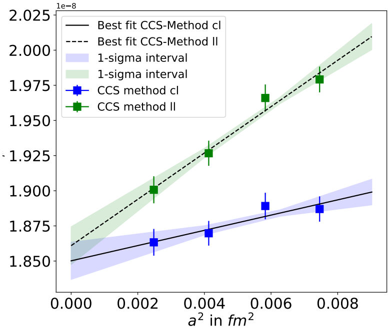

(a) Isovector contribution to a_μ^{win} at $m_\pi = 134.8$ MeV

$$(a_\mu^{\text{win}})_{\text{ll}} = (186.11 \pm 1.415) \cdot 10^{-10}$$
$$(a_\mu^{\text{win}})_{\text{cl}} = (185.008 \pm 1.398) \cdot 10^{-10}$$

TMR Mainz 22 (2206.06582):

$$a_\mu^{\text{win}} = (186.30 \pm 0.75_{\text{stat}} \pm 1.08_{\text{syst}}) \cdot 10^{-10}$$

Difference between R-Ratio and Lattice result $\sim 7 \cdot 10^{-10}$

Conclusion

Conclusion

- CCS method agrees with the TMR method in the continuum extrapolation
  - Strengthens the tension between lattice and R-ratio results
- Technical aspects
  - Behaviour of the integrand can be changed by adjusting the kernel
  - Spherical integration scheme can increase the precision on small ensembles
  - Finite Volume effects are controlled with Sakurai theory
- Outlook
  - Other observables can as well be translated to CCS representation
  - CCS representation gives a natural way of measuring observables on very large lattices (Master-field simulations)

Backup slides

Backup: Practical Aspects

O(a) Improvement

- The $O(a)$-improved vector current is given by:

$$j^I_\mu(x) = j_\mu(x) + ac_V \partial_\nu T_{\mu\nu}, \qquad \text{with} \quad T_{\mu\nu} = -\frac{1}{2}\bar{\psi}(x)[\gamma_\mu, \gamma_\nu]\psi(x) \tag{18}$$

- Using partial integration improvement term can be expressed without the need for lattice derivative

$$a_\mu^{\text{win}} = \int d^4x H_{\mu\nu}(x) G_{\mu\nu}(x) + ac_V \Big[\langle j_\mu(x) T_{\nu\alpha}(0) \rangle - \langle T_{\mu\alpha}(x) j_\nu(0) \rangle \Big] \partial_\alpha H_{\mu\nu}(x) \tag{19}$$

Backup: Practical Aspects

- For a general CCS-kernel $\widetilde{H}_{\mu\nu}(x) = -\delta_{\mu\nu}\widetilde{\mathcal{H}}_1(|x|) + \frac{x_\mu x_\nu}{|x|^2}\widetilde{\mathcal{H}}_2(|x|)$
- We only need to store data for three functions

$$G_1(r) = \sum_{|x|=r} G_{\mu\nu}(x)\delta_{\mu\nu}, \qquad G_2(r) = \sum_{|x|=r} G_{\mu\nu}(x)\frac{x_\mu x_\nu}{|x|^2} \tag{20}$$

$G_3(r) = \sum_{|x|=r} \frac{x_\alpha}{|x|^2} a c_V \Big[- \langle j_\mu(x) T_{\mu\alpha}(0)\rangle + \langle T_{\alpha\mu}(x) j_\mu(0)\rangle \Big]$ (Improvement Term)

- These functions are analogous to the spatially summed correlator in the TMR-Method $G(t) = -\frac{1}{3}\sum_{i=1}^{3} \int d^3x \langle j_i(x) j_i(0)\rangle$

Backup: Dependance of the integrand on the kernel

- Comparison of 2 different ensembles for the 3 kernel choices
- More short-ranged kernel might have oscillatory behaviour

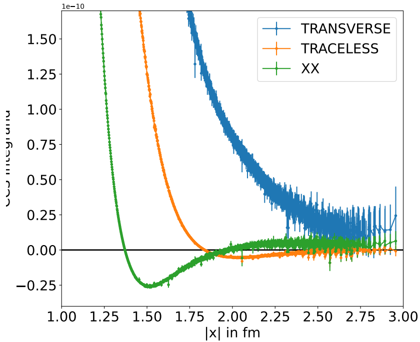

(a) N203 (L=3.1 fm)

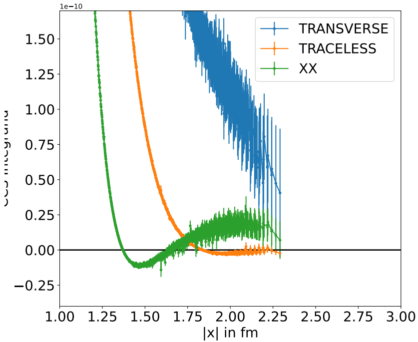

(b) N302 (L=2.4 fm)

Backup: Different Integration Schemes local-local currents

- Larger integration length improves continuum extrapolation

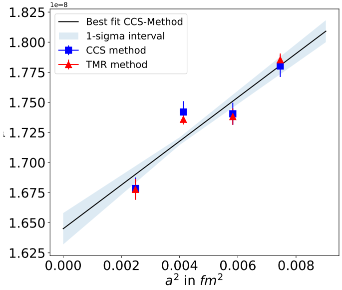

(a) Isovector contribution for local-local currents using Box Integration

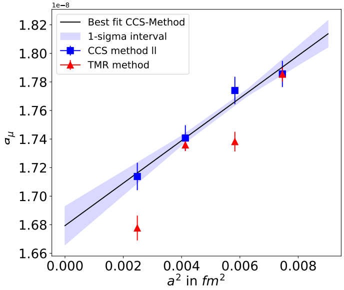

(b) Isovector contribution for local-local currents using spherical integration with correction for missing points